



Article

Electrochemical Sensors Based on Screen-Printed Electrodes: The Use of Phthalocyanine Derivatives for Application in VFA Detection

Amadou L. Ndiaye^{1,2,*}, Sébastien Delile^{1,2}, Jérôme Brunet^{1,2}, Christelle Varenne^{1,2} and Alain Pauly^{1,2}

¹ Clermont Université, Université Blaise Pascal, Institut Pascal, BP 10448, F-63000 Clermont-Ferrand, France; sebastiandelile@gmail.com (S.D.); brunet@lasmea.univ-bpclermont.fr (J.B.); christelle.VARENNE@lasmea.univ-bpclermont.fr (C.V.); Alain.PAULY@lasmea.univ-bpclermont.fr (A.P.)

² CNRS, UMR 6602, Institut Pascal, Campus Universitaire des Cézeaux, 4 Avenue Blaise Pascal, 63178 Aubiere Cedex, France

* Correspondence: amalat2005@yahoo.fr or amadou.NDIAYE@univ-bpclermont.fr; Tel.: +33-473-407-238; Fax: +33-473-407-340

Academic Editors: Donatella Albanese and Roberto Pilloton

Received: 30 May 2016; Accepted: 25 August 2016; Published: 1 September 2016

Abstract: Here, we report on the use of electrochemical methods for the detection of volatiles fatty acids (VFAs), namely acetic acid. We used tetra-tert-butyl phthalocyanine (PcH₂-tBu) as the sensing material and investigated its electroanalytical properties by means of cyclic voltammetry (CV) and square wave voltammetry (SWV). To realize the electrochemical sensing system, the PcH₂-tBu has been dropcast-deposited on carbon (C) or gold (Au) screen-printed electrodes (SPEs) and characterized by cyclic voltammetry and scanning electron microscopy (SEM). The SEM analysis reveals that the PcH₂-tBu forms mainly aggregates on the SPEs. The modified electrodes are used for the detection of acetic acid and present a linear current increase when the acetic acid concentration increases. The C modified electrode presents a limit of detection (LOD) of 25.77 mM in the range of 100 mM–400 mM, while the Au modified electrode presents an LOD averaging 40.89 mM in the range of 50 mM–300 mM. When the experiment is realized in a buffered condition, the C modified electrode presents a lower LOD, which averages the 7.76 mM. A pronounced signal decay attributed to an electrode alteration is observed in the case of the gold electrode. This electrode alteration severely affects the coating stability. This alteration is less perceptible in the case of the carbon electrode.

Keywords: dropcast-deposition; metal-free phthalocyanine; acetic acid; CV; SWV

1. Introduction

The production and optimization of renewable energy to foil global warming have gained a huge interest. Among the renewable energies, biomass-derived fuels [1–4] represent potential serious candidates, which are able to gain energy just from fermentation. Such processes give rise to the production of volatile fatty acids (VFAs) [2,4]. Among the VFAs, acetic acid (AA) represents the most abundantly-produced VFA, during controlled fermentation processes. Therefore, its monitoring is a prerequisite for optimization. For example, in biogas production, the best working conditions for an efficient gas production yield are dependent on the AA concentration [5]. Therefore, to monitor the biogas production, the acetic acid concentration is of great importance. In fact, the VFAs should be produced in a certain concentration range to ensure better performances of the reactor and simultaneously keep the pH stable [6,7]. However, recent reports show that the microbial communities are able to resist changes in the VFA concentrations [7]. Current methods employed to control such process conventionally use colorimetric and chromatographic techniques or the distillation

process [8]. However, such methods require specific encumbering equipment and expertise, which are not easy to implement.

These methods are well documented compared to electrochemical approaches, which are less explored. One reason explaining the lack of electrochemical methods dedicated to control such bio-processes is that the direct oxidation or reduction of acetic acid is very difficult to achieve in conventional electrochemistry. The only existing methods approaching the electrochemical methods are based on electrocatalytic processes. These destructive methods are based on catalytic reforming, which necessitated specific working conditions (high temperature, use of a catalyst, etc.) and suggest that the VFAs are completely transformed at the end [9–13]. All of these methods are still in use, but there is a necessity to develop new and easy to implement methods devoted to this research field.

Gaberkorn et al. [14] have studied the acid and base interaction of PcH₂ in acidic solutions (with a higher concentration of acetic acid), and they showed that the protonation of the phthalocyanine occurring mainly on the meso-nitrogen can affect the highest occupied molecular orbital (HOMO)—lowest unoccupied molecular orbital (LUMO) band gap. In this study [14], the presence of the acetic acid appears to initiate the protonation. Moreover, Stuzhin et al. [15] described some phthalocyanine and porphyrin derivatives as multicenter conjugated systems with simultaneous acid and base properties. Following these observations, we have explored the ability of the phthalocyanines as a sensing material for acetic acid detection. Taking into account that we will use concentrations lower than 0.5 M, we can surely use such phthalocyanines without inducing dissociation.

Several phthalocyanines have been investigated for applications devoted to electrocatalysis [16–18] and also for sensing purposes [19–21]. The electrochemical properties of metal-free phthalocyanines are conventionally attributed to ring redox processes, which are based on the gain or loss of electrons from their frontier orbitals [22]. Electrode modification employing phthalocyanines derivatives [23,24] has been already reported. Such a modification can, in principle, be achieved through electrodeposition [25–27], electropolymerization [20,28] and dropcasting [19]. The two first methods require specific conditions, such as the presence of an electropolymerizable group (pyrrole, thiophene etc.) [20,28] or specific working conditions [26,27]; the latter presents the advantage of being easy to perform and accessible. In fact, in the dropcasting method, the preparation of the solution in an adequate solvent can allow one to perform electrode modification. Here, we explored the dropcasting methods on screen-printed electrodes (SPEs). However, the dropcast method presents some disadvantages: (i) low film stability; (ii) the rapid ageing effect; and (iii) the non-control of the layer thickness.

Here, we studied the electrode modification of a gold and carbon working electrode using a metal-free phthalocyanine. The deposition process is achieved by the dropcast deposition method, and the successful electrode modification will be revealed through characterization of the coating using CV techniques and scanning electron microscopy techniques. Finally, the electroanalytical performance of the PcH₂-tBu-based modified electrodes towards acetic acid detection will be described by cyclic voltammetry experiments.

2. Materials and Methods

2.1. Materials and Reagents

All reagents were of analytical grade and purchased from Sigma-Aldrich. Dimethylformamide (DMF) and acetonitrile (ACN) were used as solvents without further purification. The sensing material consists of phthalocyanine derivatives, namely 2,9,16,23-tetra-tert-butyl-29H,31H-phthalocyanine (purity 97%), denoted as PcH₂-tBu. Acetic acid (AA) was purchased from Fisher and used as the analyte. Tetrabutylammonium tetrafluoroborate (TBAB), potassium chloride (KCl; 3 M), potassium dihydrogen phosphate (KH₂PO₄ salt; >99%) and potassium hydroxide (KOH; 1 M) were purchased from Sigma-Aldrich and used as electrolytes. Sulfuric acid (H₂SO₄; 0.5 M) was purchased from Fluka and used for the pretreatment of the electrodes.

2.2. Electrochemical Measurements

All measurements were carried out at room temperature. Electrochemical measurements were performed with a μ STAT 200 potentiostat (Dropsens, Oviedo, Spain) controlled by Dropview software. The electrodes consist of screen-printed electrodes (SPEs) (DRP C110 and DRP C220AT, Dropsens, Oviedo, Spain) [19,29]. The working (4 mm in diameter) and counter electrodes are made of carbon (C, DRP C110) or gold (Au, DRP C220AT), while the reference electrodes are made of silver (Ag). Such SPEs have been already used in related literature for electrode modification purposes [19,29,30]. All potentials are reported vs. the Ag pseudo-reference electrode. Cyclic voltammetry measurement were performed between -0.3 and $+0.8$ V for the gold electrodes and between -0.5 V and $+1$ V for the carbon electrodes. Square wave voltammetry was conducted between -0.3 V and $+0.4$ V with a potential step of 10 mV; a potential pulse of 60 mV and at a frequency of 15 Hz.

2.3. Solutions' Preparation

The solutions/dispersions are prepared by dissolving PcH₂-tBu in a solvent mixture (DMF/ACN (1:5 volume ratio)) containing TBAB (0.1 M) as an electrolyte. This solvent mixture was chosen to dissolve the phthalocyanine. For the electrolyte choice, TBAB was preferred to KCl, since it dissolves in organic solvent, while adding KCl solution will lead to a two-phase solution mixture, which is not suitable for deposition. The final concentration of the stock solution is 0.5 mM. Stock solutions based on PcH₂-tBu without electrolyte (TBAB) do not provide a significant electrochemical signal. The TBAB is used to enhance the conductivity in the coating (see Figure S1 in the Supporting Information). The buffered solutions (0.1 M) were prepared from KCl, KH₂PO₄ and 1 M KOH to obtain a final pH of 7.0.

2.4. Characterization of Modified Electrodes

For the characterization of the modified electrodes, cyclic voltammetry and scanning electron microscopy (SEM) were used. SEM micrographs are obtained from a Cambridge Scan 360 SEM operating at 3 kV. The samples were prepared by deposition of solution (dropcast) on the working electrodes. The coated electrodes were dried at 50 °C and were finally left overnight at room temperature.

2.5. Electrodes Modifications by Dropcasting

The deposition of the PcH₂-tBu was performed on both gold and carbon working electrodes. Prior to the deposition, the electrodes were cleaned in 0.5 M H₂SO₄ by cycling the electrode potential from -0.1 V to $+1$ V (for the Au working electrode) and from -1 V to $+1$ V (for the C working electrode) with a scan rate of 0.1 V/s. The solutions for electrode modification prepared by mixing the PcH₂tBu with solvent (see Section 2.3) were carefully deposited on the working electrodes. The coatings were dried at 50 °C and finally left overnight at room temperature.

2.6. Acetic Acid Detection Experiments

For the acetic acid (analyte) detection, KCl is used as the electrolyte. It is worth noting that TBAB can be also used as the electrolyte, but deliberately, we chose KCl for further development. In fact, KCl is used in the buffered solution [31,32] to analyze the VFA production, and in some other cases, KCl is also a component of the culture medium [33–36]. For the CV measurements, acetic acid solutions at concentrations between 0.001 M and 0.5 M containing 0.1 M KCl were prepared. To perform acetic acid detection experiments in buffered conditions, the same preparation procedure was used, except that the KCl was replaced by the buffered solution.

3. Result and Discussion

3.1. Electrode Modification by Dropcast Deposition

The dropcast deposition method is a very simple and sparing method. In fact, with a few μL of a solution, a coating can be realized. In a typical procedure of deposition, 1 μL of the stock solution ($\text{PcH}_2\text{-tBu}$; 0.5 mM) was carefully dropped onto the working electrodes (C and Au) and allowed to dry at 50 $^\circ\text{C}$ for 1 h. Care must be taken to realize the drop cast with SPEs, since the counter electrode (CE) and reference electrode (RE) are in close contact with the working electrode (WE). The CE and RE must be free of any deposit to ensure valuable electrochemical measurements. The electrodes were finally left overnight at room temperature to ensure complete solvent evaporation. The modified electrodes obtained by this procedure will be denoted *C SPE-PcH₂tBu* and *Au SPE-PcH₂tBu* in the following part of this article.

3.2. Characterization of the Modified Electrodes

To highlight the effectiveness of the coating, we have performed SEM analysis of the modified electrodes and the uncoated Au SPE for comparison. The $\text{PcH}_2\text{-tBu}$ mixture has been carefully deposited on the working electrode, and the results are shown in Figure 1.

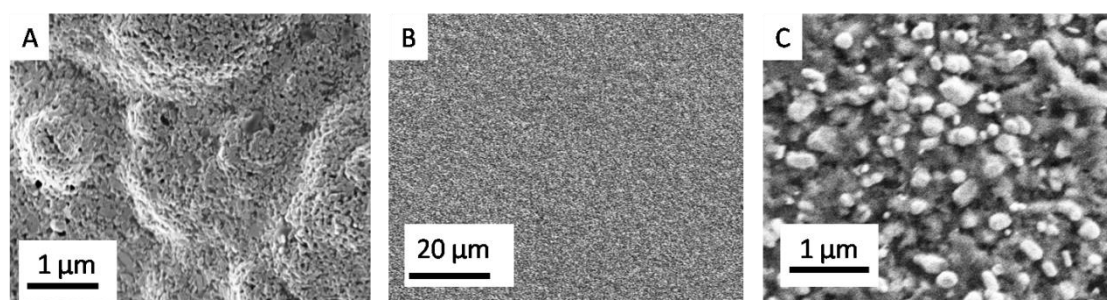


Figure 1. Representative SEM micrographs obtained before (A) and after dropcast deposition (B,C). (C) represents $\text{PcH}_2\text{-tBu}$ modified Au electrodes (B) at higher magnifications.

In the lower magnification, as displayed in Figure 1B, the $\text{PcH}_2\text{-tBu}$ appears as a relatively homogeneous layer. However, the higher magnification (Figure 1C) reveals the microstructure with a morphology close to aggregates or grain-like structures representing the $\text{PcH}_2\text{-tBu}$. The aggregates are present in different sizes and forms. The formation of aggregates is instantaneous in this liquid phase since a sonication step prior to deposition does not alter the obtained morphology. The electrolyte is embedded in the sensing layer ensuring the conductivity. Such aggregate formation is a result of the stacking formation observed in the phthalocyanine molecules.

The modified electrodes are also characterized by cyclic voltammetry. We performed cyclic voltammetry measurements of the modified electrodes in KCl (0.1 M) and compared them with CV of the bare electrodes. The results are shown in Figure 2. The *Au SPE-PcH₂tBu* presents an oxidation peak at 0.08 V and its reduction at -0.1 V, while the *C SPE-PcH₂tBu* shows an oxidation peak at 0.08 V and its reduction at -0.08 V.

Taking into consideration that bare electrodes do not present any defined peak within the electrochemical window, we can undoubtedly attribute these peaks as arising from the PcH_2tBu . These peaks are assigned to phthalocyanine ring-based redox processes [24,37,38]. The *C SPE-PcH₂tBu* modified electrode presents a quasi-reversible signal with a $\Delta E_p(E_{p,a}-E_{p,c})$ value of 160 mV, while the *Au SPE-PcH₂tBu* shows a quasi-reversible signal with a ΔE_p value of 180 mV. The $I_{p,a}/I_{p,c}$ ratios are 0.6 for *Au SPE-PcH₂tBu* and 1.9 for *C SPE-PcH₂tBu*. For both *C SPE-PcH₂tBu* and *Au SPE-PcH₂tBu* modified electrodes, the ΔE_p values are greater than 60 mV, and the $I_{p,a}/I_{p,c}$ ratios are different from one. Such behaviors suggest quasi-reversible processes. The deviation from reversibility ($I_{p,a}/I_{p,c} \neq 1$)

in these phthalocyanine-based material compounds is presumably attributed to aggregation [24], but this deviation can also reveal the existence of chemical reactions following the electrochemical ones. The formation of aggregates given through the SEM analysis corroborates such results.

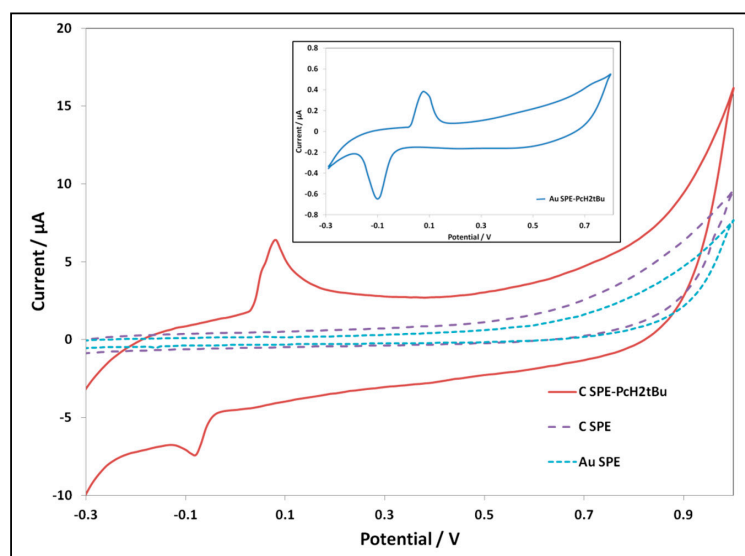


Figure 2. CV of the modified electrodes revealing the redox peaks of the PcH_2tBu in KCl 0.1 M at a scan rate of 0.1 V/s. For comparison, the CV of the bare electrodes on the same KCl solution is shown. Inset: CV of Au SPE- PcH_2tBu is represented in the inset, due to the low current intensity range.

3.3. Acetic Acid Detection

Figure 3 shows the CV response of the *Au SPE-PcH₂tBu* at different acid concentrations. At an acetic acid concentration of 50 mM, the *Au SPE-PcH₂tBu* presents peaks that are localized at 0.11 V and −0.09 V. These peaks are slightly shifted compared to that obtained in pure electrolyte solution (represented by AA 0 mM in Figure 3).

By progressively increasing the amount of acetic acid, we observed a current increase as a function of the acid concentration. At a higher acid concentration, the oxidation peak is broadened, while the reduction peak seems to split into two peaks. This can be interpreted as resulting from an associated chemical reaction that occurs at a higher acid concentration. Moreover, up to 300 mM, the *Au SPE-PcH₂tBu* electrode saturates. The broadening of the oxidation peaks combined with the occurrence of the splitting in the reduction side, at a higher acid concentration, can be associated with a chemical reaction occurring at a higher concentration and certainly leading to the modification of the structure. The calibration curve given in the inset of Figure 3 presents the linear dependence of the current intensity with concentration. From the calibration curve (inset in Figure 3), we can evaluate the limit of detection (LOD), which can be calculated following the $3\text{SD}/m$ criterion [39], where m is the slope of the calibration graph and SD is the standard deviation of the voltammetric signal at the lowest concentration. We have calculated an LOD of 40.89 mM from the anodic peak at ca. +0.11 V.

In the case of *C SPE-PcH₂tBu*, a different trend is observed. Figure 4 represents the CV of the modified electrode upon the addition of acetic acid. Here, the concentration range is from 100 mM–400 mM, since at a concentration lower than 100 mM, the signal is unclear. At an acetic acid concentration of 100 mM, the *C SPE-PcH₂tBu* presents peaks that are localized at 0.1 V and −0.1 V. These peaks are again shifted compared to those obtained in KCl. The calibration curve given in the inset of Figure 4 presents the linear dependence of the current intensity with concentration. In the case of *C SPE-PcH₂tBu*, the linear dependence is more accurate, as illustrated by the value of correlation coefficient R^2 of 0.999. From the calibration curve, we have calculated an LOD of 25.77 mM from the anodic peak at ca. +0.10 V.

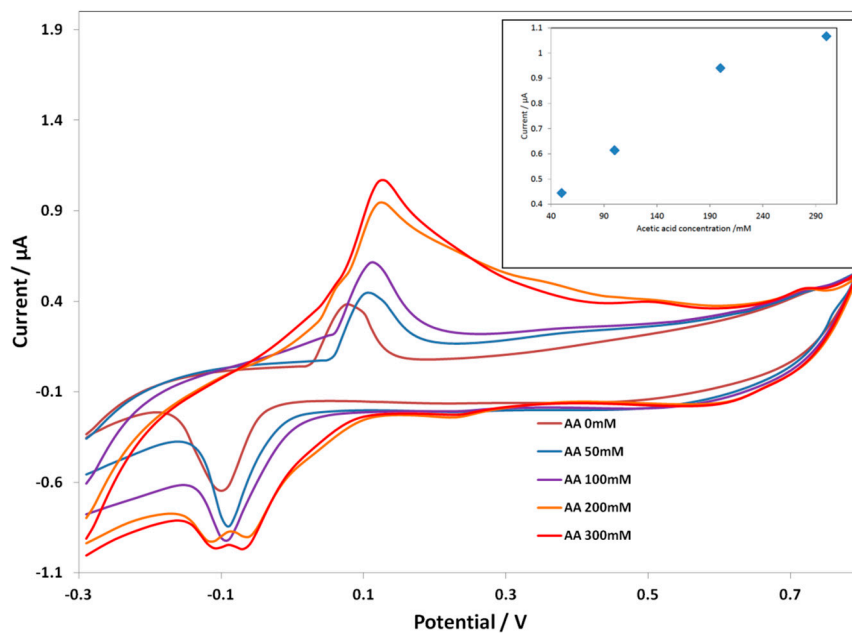


Figure 3. CV curves of Au screen-printed electrode(SPE)-PcH₂tBu with the addition of the acetic acid in 0.1 M KCl. The CV labeled AA 0 mM represents the experiment in pure electrolyte (0.1 M KCl). Scan rate = 0.1 V/s.

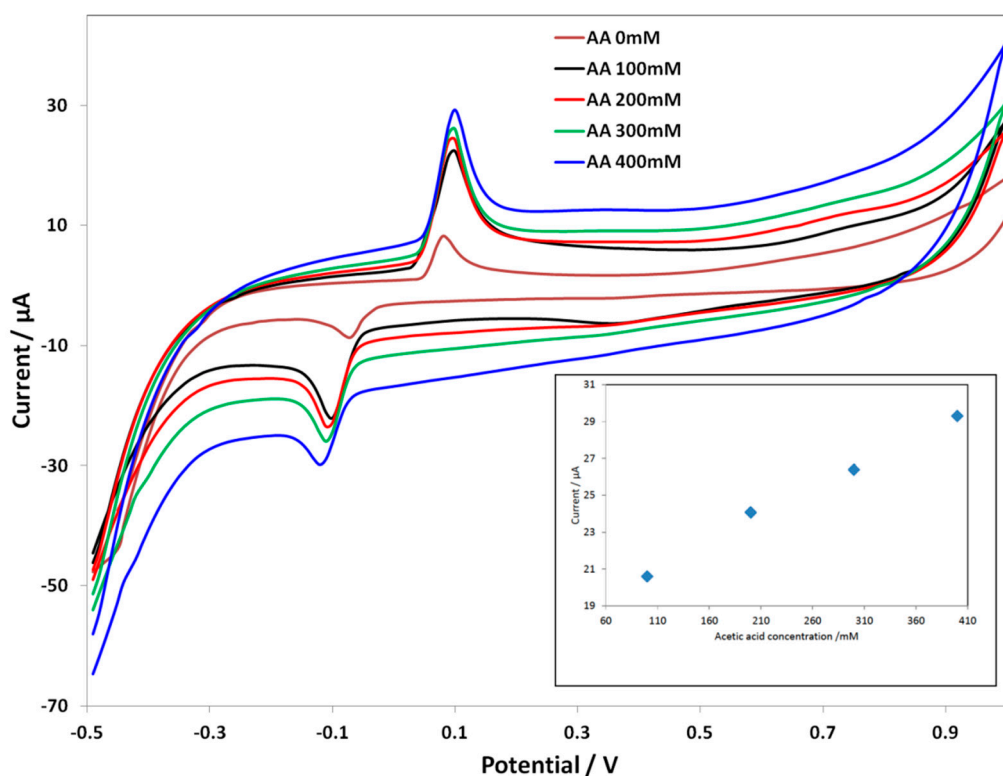


Figure 4. CV curves of C SPE-PcH₂tBu with the addition of the acetic acid in 0.1 M KCl. The CV labeled AA 0 mM represents the experiment in pure electrolyte (0.1 M KCl). Scan rate = 0.1 V/s.

In both cases (*C SPE-PcH₂tBu* and *Au SPE-PcH₂tBu*), current versus concentration analysis revealed a linear dependence between the current peak and the analyte concentration. The different LOD values are attributed to the different electrocatalytic activity of the different electrodes. Even if

this concentration range is currently high and the LOD in the mM range, these results show that such modified electrodes can be used for acid acetic detection.

We have also evaluated the reproducibility and the lifetime of the electrochemical sensors. For this study, a solution containing 100 mM acetic acid has been used in successive experiments. A general current signal decreasing is shown, and this effect is more pronounced in the Au electrode. Indeed, the percentage of current decay is around 20%, based on 30 experiments, when gold is used as the working electrode, while this value averages 10% for the carbon electrodes. After several experiments, also new peaks coming probably from the Au electrodes' oxidation are identified for the *Au SPE-PcH₂tBu*. In summary, after 40–50 experiments, the sensors show a general alteration, which is characterized by a pronounced flattening of the current peaks. The lifetime has been set to 50 CV cycles. This effect is more accelerated when higher acetic acid concentrations are used. Therefore, the lifetime of 50 CV is only valid if we work in the above-mentioned conditions. The deposit seems to be more efficient on the carbon electrode compared to the gold electrode. Taking into account that the carbon electrode contains graphitic layers, we can explain this behavior by the possibility of the PcH₂tBu to interact with the carbon electrode via the π – π interaction in a manner similar to the non-covalent interaction between carbon nanotubes and phthalocyanine derivatives [40].

Since the C modified electrodes were more stable, we performed an experiment with the *C SPE-PcH₂tBu* to check the electroanalytical performance in buffered solutions by both the CV and SWV techniques. To this end, acetic acid has been added to a 0.1 M buffered solution (see the experimental part) to reach a concentration between 10 mM and 300 mM. The results are presented in Figure 5 (for the CV) and Figure 6 (for SWV). At the acetic acid concentration of 10 mM, the *C SPE-PcH₂tBu* presents peaks that are localized at +0.09 V and –0.08 V. We can notice that, in the buffered condition, the lowest attainable concentration giving an electrochemical signal is 10 mM by CV, while this value attains 25 mM by SWV. However, a broadening of the CV peaks occurs in buffered media compared to the peaks obtained in unbuffered media. This is explained by the high background current, which is exalted in the buffered media.

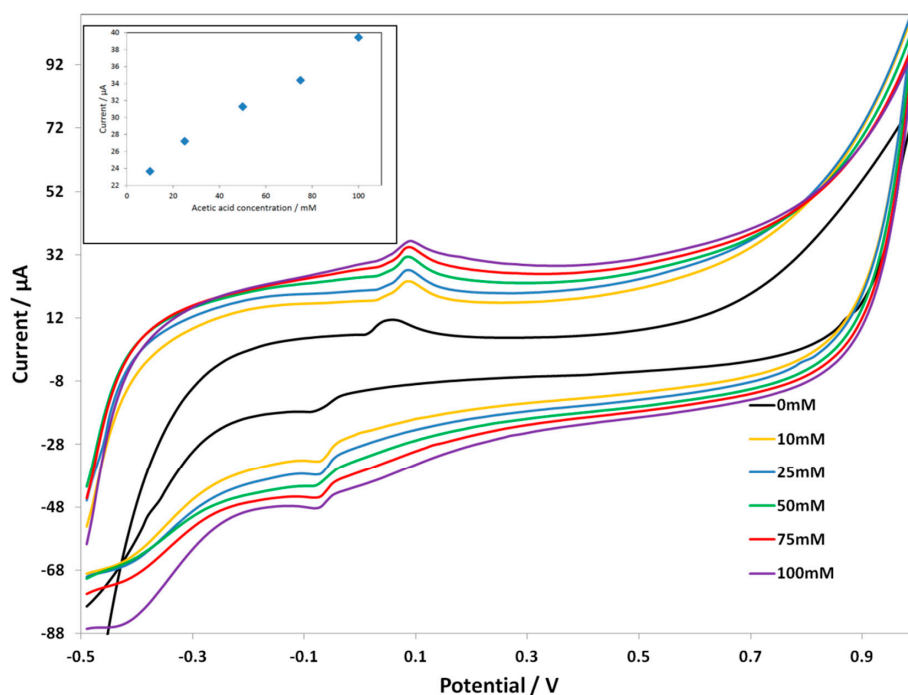


Figure 5. CV curves of C SPE-PcH₂tBu with the addition of the acetic acid in 0.1 M buffer solution. The CV labeled AA 0 mM represents the experiment in pure electrolyte. Scan rate = 0.1 V/s.

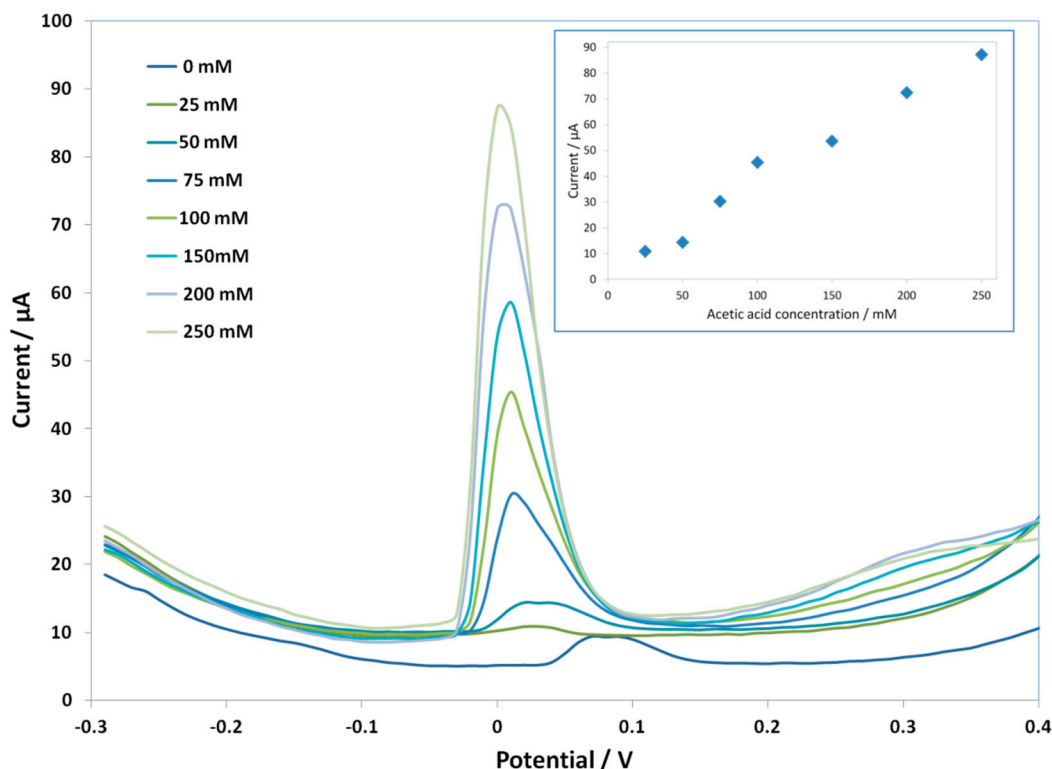


Figure 6. SWV curves of C SPE-PcH₂tBu with the addition of the acetic acid in 0.1 M buffer solution. Potential step = 10 mV; potential pulse = 60 mV; frequency = 15 Hz. The SWV curve labeled as 0 mM represents the experiment in pure electrolyte. The insert shows the current dependence with the acetic acid concentration.

The sensor displays a linear response to acetic acid in the range of 10 mM–100 mM (inset in Figure 5) with a correlation coefficient R^2 of 0.99. We obtained an LOD of 7.76 mM from the anodic peak at ca. +0.09 V. This result shows that the modified electrodes can be used in buffered, as well as in unbuffered media; a result that will be useful for further development in bioreactors.

We have also performed SWV experiment on the C SPE-PcH₂tBu for the acetic acid detection. The SWV parameters have been optimized (see the caption of Figure 6) and used for recording the SWV current signal. The SWV responses are displayed in Figure 6, and the insert contains the SWV current evolution as a function of the acetic acid concentration. We depicted, from these results, a current increase upon increasing the acid concentration. The SWV results are concomitant with those observed in the acetic acid detection using CV techniques. The responses are clearly identified, but the increase in the signal is still low. Nevertheless, we can clearly depict a shift between only KCl solution and acetic acid-containing solutions. This shift is more clearly evidenced than in the CV methods.

At this stage, it would be interesting to compare the electroanalytical performance of our modified electrodes to other electrochemical system in terms of the sensing of acetic acid. However, in front of the poor number of articles or reports dealing with acid acetic detection using electrochemical methods, we are unable to provide a valuable comparison.

After performing the evaluation of the sensing performance, we have also conducted sensing experiments on the modified electrodes to characterize the redox process taking place in such modified electrodes. Therefore, we recorded the evolution of the current peak while increasing the scan rate of the modified electrodes in the presence of the analyte. This study has been conducted in a 100 mM acetic acid solution containing 100 mM KCl with a scan rate from 25–500 mV/s. Figure 7 shows the evolution of the anodic current peak as a function of the increasing scan rate.

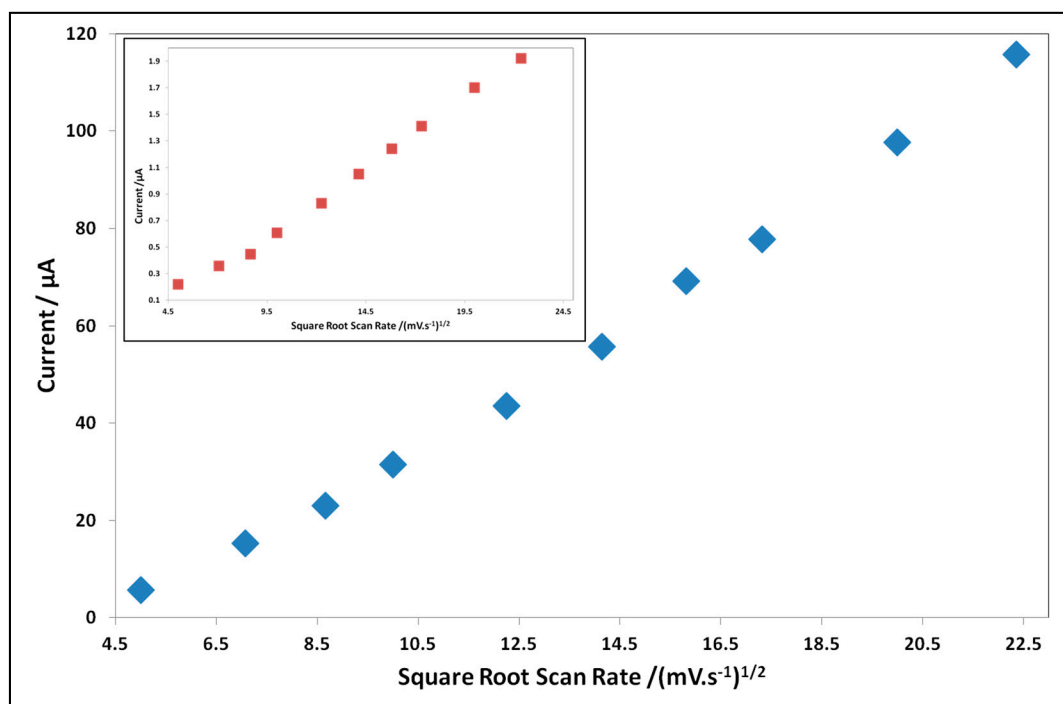


Figure 7. The evolution of current peak of the modified electrodes upon increasing the scan rate in 100 mM acetic acid solution. Due to the difference in the current range, the case of *Au SPE-PcH₂tBu* is displayed in the inset.

An increasing potential scan rate gives rise to an increase of the current peak as shown in Figure 7 for all modified electrodes. The *PcH₂tBu* modified electrodes show a linear dependence of the anodic peak current with the square root of the scan rate. The linearity dependence is also confirmed by the regression coefficient (R^2) value ($R^2 = 0.994$ for *C SPE-PcH₂tBu* and $R^2 = 0.995$ for *Au SPE-PcH₂tBu*) and is indicative of a predominant diffusion-controlled redox process. The difference in slopes is attributed to the difference in the nature of the electrode material.

Taking into account that the potential peaks in phthalocyanine and porphyrin derivatives are attributed to the electron's promotion from the HOMO or LUMO energy levels, the presence of the acid will induce a perturbation on the delocalized pi-electrons (through protonation or coordination), which will be translated into a change on the HOMO/LUMO band gap positioning. In fact, the spectroscopic studies by Gaberkorn et al. [14] in the case of the *PcH₂* have revealed that protonation induces a change in the HOMO/LUMO band gap positioning, causing a shift in UV-visible spectra. In the protonated or unprotonated form, the *PcH₂tBu* can also interact with the acetate anion, which is a highly coordinating ligand. Taking into account the previous studies about phthalocyanines and the acid base interaction [14,15,41], we have proposed a two-step mechanism: (i) a first step leading to a protonation; (ii) and the subsequent coordination of the analyte (acetate form or acetic form). However, the fact that protonation induces a change can be regarded as a drawback since other inorganic acids (different from VFA) will also induce a similar change, and this effect will point to a lack of selectivity. However, taking into account that acetic acid is the most abundantly-produced in bioreactors, its detection can be useful to control the monitoring of the whole VFA production. Even if the protonation is the first step in the mechanism, the coordination of the carboxyl and carboxylate group to the macrocycle center containing a delocalized π -system is responsible for the response observed. This behavior is confirmed by the responses recorded in buffered media by both CV and SWV experiments.

4. Conclusions

Here, we investigated the possibility to modify SPEs with metal-free phthalocyanine for acetic acid detection by the dropcast method. The electrode modification processed through dropcast deposition is a simple and sparing method, which presents serious potential for further development in the field acetic acid detection. Their characterization by cyclic voltammetry and SEM analysis, as well as the evaluation of their electroanalytical performances have shown the effectiveness of such electrodes' modification and their potential use for electrochemical detection. The carbon electrodes present a high background current, but allow to obtain stable electrodes. On the contrary, the gold electrode, which seems to be well suited for electroanalytical experiments, presents some limits (oxidation, stability). We showed here that these modified electrodes can be used to detect acetic acid. The detected concentration is currently limited in the mM range, but we intend to improve the process and to lower the detection limit in further investigation. This work opens a new window on the utilization of macrocycle-based material for acid acetic detection and proposes new ideas for VFA detection.

Acknowledgments: This work has been sponsored by the French government research program “Investissements d’avenir” through the IMobS3 Laboratory of Excellence (ANR-10-LABX-16-01), by the European Union through the program Regional competitiveness and employment 2007–2013 (ERDF-Auvergne region) and by the Auvergne region. We thank Maria Luz. Rodríguez-Méndez for its helpful suggestions in the VFA research project.

A.L. Ndiaye and S. Delile thank the “Laboratoire d’Excellence IMobS3” for postdoctoral fellowships. J. Brunet, A. Pauly and A.L. Ndiaye would like to thank the transdisciplinary COST Action TD 1105 “EuNetAir”, in which they are involved, for supporting these scientific activities.

Author Contributions: A.L.N., A.P. and S.D. conceived and designed the experiments; A.L.N. performed the experiments; A.P., J.B. and C.V. analyzed the data; A.L.N. and S.D. contributed reagents/materials/analysis tools; A.L.N. wrote the paper.

Conflicts of Interest: The authors declare that there is no conflict of interest.

References

1. Pind, P.F.; Angelidaki, I.; Ahring, B.K. Dynamics of the anaerobic process: Effects of volatile fatty acids. *Biotechnol. Bioeng.* **2003**, *82*, 791–801. [[CrossRef](#)] [[PubMed](#)]
2. Zhou, A.; Guo, Z.; Yang, C.; Kong, F.; Liu, W.; Wang, A. Volatile fatty acids productivity by anaerobic co-digesting waste activated sludge and corn straw: Effect of feedstock proportion. *J. Biotechnol.* **2013**, *168*, 234–239. [[CrossRef](#)] [[PubMed](#)]
3. Appels, L.; Assche, A.V.; Willems, K.; Degreève, J.; Impe, J.V.; Dewil, R. Peracetic acid oxidation as an alternative pre-treatment for the anaerobic digestion of waste activated sludge. *Bioresour. Technol.* **2011**, *102*, 4124–4130. [[CrossRef](#)] [[PubMed](#)]
4. Chang, H.; Kim, N.-J.; Kang, J.; Jeong, C. Biomass-Derived volatile fatty acid platform for fuels and chemicals. *Biotechnol. Bioproc. Eng.* **2010**, *15*, 1–10. [[CrossRef](#)]
5. Greetham, D. Presence of low concentrations of acetic acid improves fermentations using *saccharomyces cerevisiae*. *J. Bioprocess. Biotech.* **2014**, *5*, 192.
6. Lahav, O.; Morgan, B.E. Titration methodologies for monitoring of anaerobic digestion in developing countries—A review. *J. Chem. Technol. Biotechnol.* **2004**, *79*, 1331–1341. [[CrossRef](#)]
7. Franke-Whittle, I.H.; Walter, A.; Ebner, C.; Insam, H. Investigation into the effect of high concentrations of volatile fatty acids in anaerobic digestion on methanogenic communities. *Waste Manag.* **2014**, *34*, 2080–2089. [[CrossRef](#)] [[PubMed](#)]
8. Lahav, O.; Morgan, B.E.; Loewenthal, R.E. Rapid, simple, and accurate method for measurement of VFA and carbonate alkalinity in anaerobic reactors. *Environ. Sci. Technol.* **2002**, *36*, 2736–2741. [[CrossRef](#)] [[PubMed](#)]
9. Chen, Y.; Yuan, L.; Ye, T.; Qiu, S.; Zhu, X.; Torimoto, Y.; Yamamoto, M.; Li, Q. Effects of current upon hydrogen production from electrochemical catalytic reforming of acetic acid. *Int. J. Hydrogen Energy* **2009**, *34*, 1760–1770. [[CrossRef](#)]
10. Barbier, J., Jr.; Delanoë, F.; Jabouille, F.; Duprez, D.; Blanchard, G.; Isnard, P. Total oxidation of acetic acid in aqueous solutions over noble metal catalysts. *J. Catal.* **1998**, *177*, 378–385. [[CrossRef](#)]

11. Nonaka, H.; Matsumura, Y. Electrochemical oxidation of carbon monoxide, methanol, formic acid, ethanol, and acetic acid on a platinum electrode under hot aqueous conditions. *J. Electroanal. Chem.* **2002**, *520*, 101–110. [[CrossRef](#)]
12. Hoang, T.M.C.; Geerdink, B.; Sturm, J.M.; Lefferts, L.; Seshan, K. Steam reforming of acetic acid—A major component in the volatiles formed during gasification of humin. *Appl. Catal. B Environ.* **2015**, *163*, 74–82. [[CrossRef](#)]
13. Nogueira, F.G.E.; Assaf, P.G.M.; Carvalho, H.W.P.; Assaf, E.M. Catalytic steam reforming of acetic acid as a model compound of bio-oil. *Appl. Catal. B Environ.* **2014**, *160–161*, 188–199. [[CrossRef](#)]
14. Gaberkorn, A.A.; Popkova, I.A.; Stuzhin, P.A.; Ercolani, C. Study of basic properties of tert-butyl-substituted tribenzo(1,2,5-thiadiazolo)porphyrazines. *Russ. J. Gen. Chem.* **2006**, *76*, 1494–1503. [[CrossRef](#)]
15. Stuzhin, P.A. Azaporphyrins and phthalocyanines as multicentre conjugated ampholites. *J. Porphyr. Phthalocyanines* **1999**, *03*, 500–513. [[CrossRef](#)]
16. Trevin, S.; Bedioui, F.; Guadalupe Gomez Villegas, M.; Bied-Charreton, C. Electropolymerized nickel macrocyclic complex-based films: Design and electrocatalytic application. *J. Mater. Chem.* **1997**, *7*, 923–928. [[CrossRef](#)]
17. Seelan, S.; Sinha, A.K.; Srinivas, D.; Sivasanker, S. Spectroscopic investigation and catalytic activity of copper(ii) phthalocyanine encapsulated in zeolite y. *J. Mol. Catal. A Chem.* **2000**, *157*, 163–171. [[CrossRef](#)]
18. Zagal, J.H.; Griveau, S.; Silva, J.F.; Nyokong, T.; Bedioui, F. Metallophthalocyanine-based molecular materials as catalysts for electrochemical reactions. *Coord. Chem. Rev.* **2010**, *254*, 2755–2791. [[CrossRef](#)]
19. Matemadombo, F.; Apetrei, C.; Nyokong, T.; Rodríguez-Méndez, M.L.; de Saja, J.A. Comparison of carbon screen-printed and disk electrodes in the detection of antioxidants using copc derivatives. *Sens. Actuators B Chem.* **2012**, *166–167*, 457–466. [[CrossRef](#)]
20. Bedioui, F.; Devynck, J.; Bied-Charreton, C. Immobilization of metalloporphyrins in electropolymerized films: Design and applications. *Accounts Chem. Res.* **1995**, *28*, 30–36. [[CrossRef](#)]
21. Arrieta, A.; Rodriguez-Mendez, M.L.; de Saja, J.A. Langmuir–Blodgett film and carbon paste electrodes based on phthalocyanines as sensing units for taste. *Sens. Actuators B Chem.* **2003**, *95*, 357–365. [[CrossRef](#)]
22. Lever, A.B.P.; Milaeva, E.R.; Speier, G. *Phthalocyanines, Properties and Application*; Leznoff, C.C., Lever, A.B.P., Eds.; VCH Publishers: New York, NY, USA, 1993; Volume 3.
23. Li, H.; Guarr, T.F. Formation of electronically conductive thin films of metal phthalocyanines via electropolymerization. *J. Chem. Soc. Chem. Commun.* **1989**, 832–834. [[CrossRef](#)]
24. Bıyıklıođlu, Z.; akır, V.; Demir, F.; Koca, A. New electropolymerizable metal-free and metallophthalocyanines bearing {2-[3-(diethylamino)phenoxy]ethoxy} substituents. *Synth. Metals* **2014**, *196*, 166–172. [[CrossRef](#)]
25. Peeters, K.; De Wael, K.; Vincze, L.; Adriaens, A. Comparison of different surface modification techniques for electrodes by means of electrochemistry and micro synchrotron radiation x-ray fluorescence. Dimerization of cobalt(ii) tetrasulfonated phthalocyanine and its influence on the electrodeposition on gold surfaces. *Anal. Chem.* **2005**, *77*, 5512–5519. [[PubMed](#)]
26. De Wael, K.; Westbroek, P.; Adriaens, A.; Temmerman, E. Role of gold adatoms in the stability and electrochemical behavior of gold surfaces modified with phthalocyanines. *Electrochim. Solid-State Lett.* **2005**, *8*, C65–C68. [[CrossRef](#)]
27. Ilangovan, G.; Zweier, J.L.; Kuppasamy, P. Electrochemical preparation and epr studies of lithium phthalocyanine: Evaluation of the nucleation and growth mechanism and evidence for potential-dependent phase formation. *J. Phys. Chem. B* **2000**, *104*, 4047–4059. [[CrossRef](#)]
28. Sehlotho, N.; Nyokong, T.; Zagal, J.H.; Bedioui, F. Electrocatalysis of oxidation of 2-mercaptoethanol, l-cysteine and reduced glutathione by adsorbed and electrodeposited cobalt tetra phenoxy pyrrole and tetra ethoxy thiophene substituted phthalocyanines. *Electrochim. Acta* **2006**, *51*, 5125–5130. [[CrossRef](#)]
29. Conzuelo, F.; Gamella, M.; Campuzano, S.; Reviejo, A.J.; Pingarr3n, J.M. Disposable amperometric magneto-immunosensor for direct detection of tetracyclines antibiotics residues in milk. *Anal. Chim. Acta* **2012**, *737*, 29–36. [[CrossRef](#)] [[PubMed](#)]
30. Pellicer, C.; Gomez-Caballero, A.; Unceta, N.; Goicolea, M.A.; Barrio, R.J. Using a portable device based on a screen-printed sensor modified with a molecularly imprinted polymer for the determination of the insecticide fenitrothion in forest samples. *Anal. Methods* **2010**, *2*, 1280–1285. [[CrossRef](#)]

31. Christophe, G.; Kumar, V.; Nouaille, R.; Gaudet, G.; Fontanille, P.; Pandey, A.; Soccol, C.R.; Larroche, C. Recent developments in microbial oils production: A possible alternative to vegetable oils for biodiesel without competition with human food? *Brazilian Arch. Biol. Technol.* **2012**, *55*, 29–46. [[CrossRef](#)]
32. Jin, X.; Angelidaki, I.; Zhang, Y. Microbial electrochemical monitoring of volatile fatty acids during anaerobic digestion. *Environ. Sci. Technol.* **2016**, *50*, 4422–4429. [[CrossRef](#)] [[PubMed](#)]
33. Sträuber, H.; Bühligen, F.; Kleinstauber, S.; Nikolausz, M.; Porsch, K. Improved anaerobic fermentation of wheat straw by alkaline pre-treatment and addition of alkali-tolerant microorganisms. *Bioengineering* **2015**, *2*, 66. [[CrossRef](#)]
34. Ghosh, A.; Bhattacharyya, C.B. Biomethanation of white rotted and brown rotted rice straw. *Bioprocess Eng.* **1999**, *20*, 297–302. [[CrossRef](#)]
35. Somasiri, W.; Li, X.-F.; Ruan, W.-Q.; Jian, C. Evaluation of the efficacy of upflow anaerobic sludge blanket reactor in removal of colour and reduction of cod in real textile wastewater. *Bioresour. Technol.* **2008**, *99*, 3692–3699. [[CrossRef](#)] [[PubMed](#)]
36. Antonopoulou, G.; Stamatelatou, K.; Venetsaneas, N.; Kornaros, M.; Lyberatos, G. Biohydrogen and methane production from cheese whey in a two-stage anaerobic process. *Ind. Eng. Chem. Res.* **2008**, *47*, 5227–5233. [[CrossRef](#)]
37. Bıyıklıoğlu, Z.; Çakır, D. New electropolymerizable metal-free and metallophthalocyanines bearing {2,3-bis[3-(diethylamino)phenoxy]propoxy} substituents. *Dyes Pigment.* **2014**, *100*, 150–157. [[CrossRef](#)]
38. Çakır, V.; Demir, F.; Bıyıklıoğlu, Z.; Koca, A.; Kantekin, H. Synthesis, characterization, electrochemical and spectroelectrochemical properties of metal-free and metallophthalocyanines bearing electropolymerizable dimethylamine groups. *Dyes Pigment.* **2013**, *98*, 414–421. [[CrossRef](#)]
39. Medina-Plaza, C.; García-Cabezón, C.; García-Hernández, C.; Bramorski, C.; Blanco-Val, Y.; Martín-Pedrosa, F.; Kawai, T.; de Saja, J.A.; Rodríguez-Méndez, M.L. Analysis of organic acids and phenols of interest in the wine industry using langmuir–blodgett films based on functionalized nanoparticles. *Anal. Chim. Acta* **2015**, *853*, 572–578. [[CrossRef](#)] [[PubMed](#)]
40. Ndiaye, A.; Bonnet, P.; Pauly, A.; Dubois, M.; Brunet, J.; Varenne, C.; Guerin, K.; Lauron, B. Noncovalent functionalization of single-wall carbon nanotubes for the elaboration of gas sensor dedicated to btx type gases: The case of toluene. *J. Phys. Chem. C* **2013**, *117*, 20217–20228. [[CrossRef](#)]
41. Berezin, B.D.; Shukhto, O.V.; Berezin, D.B. A new type of metal porphyrin dissociation reaction. *Russ. J. Inorg. Chem.* **2002**, *47*, 1763–1768.



© 2016 by the authors; licensee MDPI, Basel, Switzerland. This article is an open access article distributed under the terms and conditions of the Creative Commons Attribution (CC-BY) license (<http://creativecommons.org/licenses/by/4.0/>).